Article
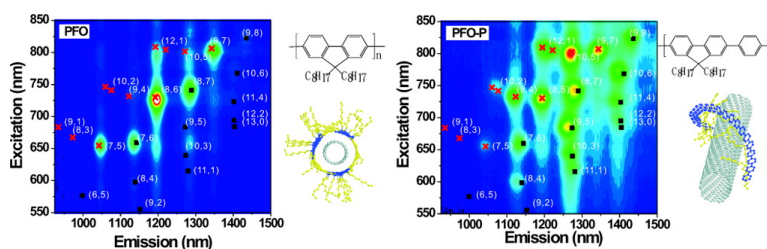
Polymer Structure and Solvent Effects on the Selective Dispersion of Single-Walled Carbon Nanotubes

Jeong-Yuan Hwang, Adrian Nish, James Doig, Sigrid Douven,
Chun-Wei Chen, Li-Chyong Chen, and Robin J. Nicholas

More About This Article

Additional resources and features associated with this article are available within the HTML version:

- Supporting Information
- Links to the 4 articles that cite this article, as of the time of this article download
- Access to high resolution figures
- Links to articles and content related to this article
- Copyright permission to reproduce figures and/or text from this article

View the Full Text HTML

Polymer Structure and Solvent Effects on the Selective Dispersion of Single-Walled Carbon Nanotubes

Jeong-Yuan Hwang,[†,‡,§] Adrian Nish,[†] James Doig,[†] Sigrid Douven,[‖]
Chun-Wei Chen,[‡] Li-Chyong Chen,[§] and Robin J. Nicholas*,[†]

*Clarendon Laboratory, Parks Road, Oxford University OX1 3PU, U.K., Department of Materials
Science and Engineering, National Taiwan University, Taipei 10617, Taiwan, Centre for
Condensed Matter Sciences, National Taiwan University, Taipei 10617, Taiwan, and Department
of Chemical Engineering, Université de Liège, 3 Allée de la chimie, 4000 Liège, Belgium*

Received October 9, 2007; E-mail: r.nicholas@physics.ox.ac.uk

Abstract: Combinations of different aromatic polymers and organic solvents have been studied as dispersing agents for preparing single-walled carbon nanotubes solutions, using optical absorbance, photolumines-cence-excitation mapping, computer modeling, and electron microscopic imaging to characterize the solutions. Both the polymer structure and solvent used strongly influence the dispersion of the nanotubes, leading in some cases to very high selectivity in terms of diameter and chiral angle. The highest selectivities are observed using toluene with the rigid polymers PFO-BT and PFO to suspend isolated nanotubes. The specific nanotube species selected are also dependent on the solvent used and can be adjusted by the use of THF or xylene. Where the structure has more flexible conformations, the polymers are shown to be less selective but show an enhanced overall solubilization of nanotube material. When chloroform is used as the solvent, there is a large increase in the overall solubilization, but the nanotubes are suspended as bundles rather than as isolated tubes which leads to a quenching of their photoluminescence.

Introduction

Since the discovery of single-walled carbon nanotubes (SWNTs), their excellent mechanical and electrical properties have made them promising materials for many potential applications.[1-4] The wrapping of the graphene sheet leads to many distinct possible structures, defined by the chiral indices n and m,[5] with a third of the species being metallic and the remainder being semiconducting. However, raw SWNT samples are usually dominated by bundles of tubes, with the distribution of tube structures depending on the preparation method.[6-10] The diversity of tube diameters, chiral angles, and aggregation makes their useful application difficult. It is thus desirable to find ways

to separate metallic from semiconducting tubes or, further, to be able to purify down to a unique species with specific electrical properties from a given SWNT material.

The dispersion of SWNTs in solutions is useful for their analysis, purification, and modification. Several methods of solubilizing SWNTs through chemical and physical function-alization have been reported. Although chemical functionaliza-tion[11-15] significantly enhances solubilization of SWNTs in various solvents, it also changes the intrinsic properties of the SWNTs due to the modification of their graphene surfaces. Therefore, noncovalent functionalization through polymer wrap-ping[16] or adsorption of ionic surfactants[17-19] enables dispersion, while preserving the intrinsic properties of the SWNT. Of these methods, $\pi-\pi$ stacking[20,21] is of interest because interactions
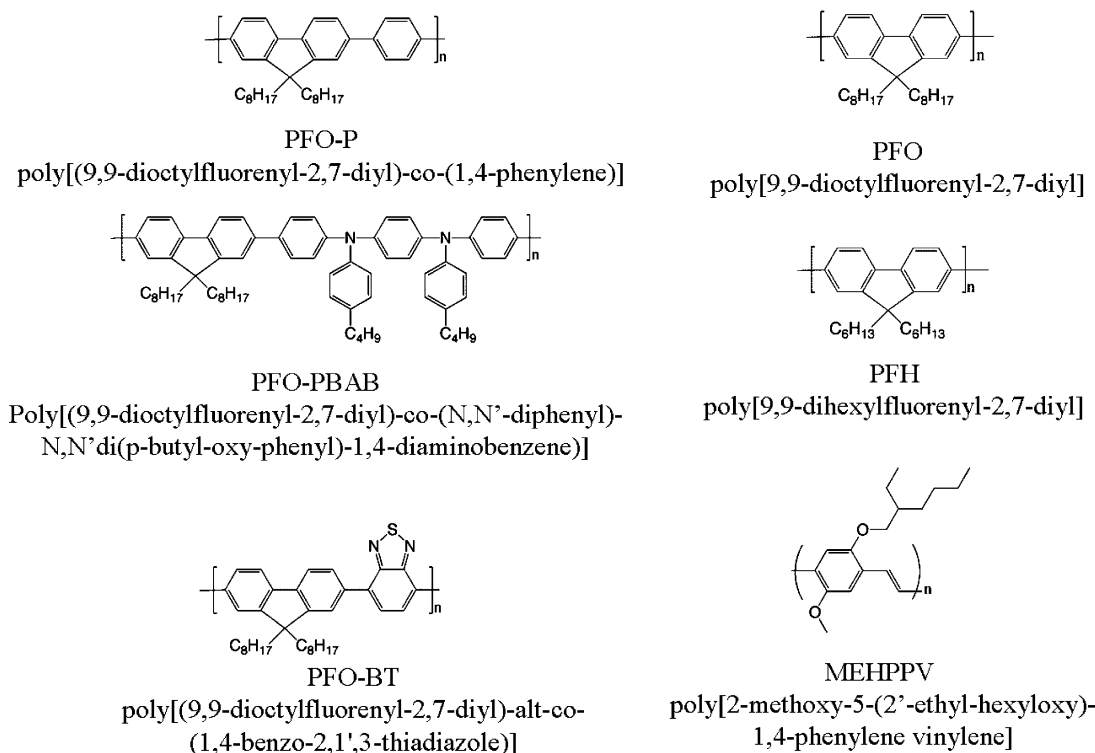
[†] Oxford University.
[‡] Department of Materials Science and Engineering, National Taiwan University.
[§] Centre for Condensed Matter Sciences, National Taiwan University.
[‖] Université de Liège.

(1) Iijima, S.; Ichihashi, T. *Nature* **1993**, *363*, 603.
(2) Bethune, D. S.; Klang, C. H.; de Vries, M. S.; Gorman, G.; Savoy, R.; Vazquez, J.; Beyers, R. *Nature* **1993**, *363*, 605.
(3) Niyogi, S.; Hamon, M. A.; Hu, H.; Zhao, B.; Bhowmik, P.; Sen, R.; Itkis, M. E.; Haddon, R. C. *Acc. Chem. Res.* **2002**, *35*, 1105.
(4) Dresselhaus, M. S.; Dresselhaus, G.; Avouris, P. *Carbon Nanotubes: Synthesis, Structure, Properties, and Applications*; Springer: Berlin, 2001.
(5) Saito, R.; Fujita, M.; Dresselhaus, G.; Dresselhaus, M. S. *Appl. Phys. Lett.* **1992**, *60*, 2204.
(6) Journet, C.; Maser, W. K.; Bernier, P.; Loiseau, A.; delaChapelle, M. L.; Lefrant, S.; Deniard, P.; Lee, R.; Fischer, J. E. *Nature* **1997**, *388*, 756.
(7) Bachilo, S. M.; Strano, M. S.; Kittrell, C.; Hauge, R. H.; Smalley, R. E.; Weisman, R. B. *Science* **2002**, *298*, 2361.
(8) Bachilo, S. M.; Balzano, L.; Herrera, J. E.; Pompeo, F.; Resasco, D. E.; Weisman, R. B. *J. Am. Chem. Soc.* **2003**, *125*, 11186.
(9) Kukovecz, A.; Kramberger, C.; Georgakilas, V.; Prato, M.; Kuzmany, H. *Eur. Phys. J. B* **2002**, *28*, 223.
(10) An, L.; Owens, J. M.; McNeil, L. E.; Liu, J. *J. Am. Chem. Soc.* **2002**, *124*, 13688.
(11) Chen, J.; Hamon, M. A.; Hu, H.; Chen, Y. S.; Rao, A. M.; Eklund, P. C.; Haddon, R. C. *Science* **1998**, *282*, 95.
(12) Boul, P. J.; Liu, J.; Michelson, E. T.; Huffman, C. B.; Ericson, L. M.; Chiang, I. W.; Smith, K. A.; Colbert, D. T.; Hauge, R. H.; Margrave, J. L.; Smalley, R. E. *Chem. Phys. Lett.* **1999**, *310*, 367.
(13) Zhao, B.; Hu, H.; Niyogi, S.; Itkis, M. E.; Hamon, M. A.; Bhowmik, P.; Meier, M. S.; Haddon, R. C. *J. Am. Chem. Soc.* **2001**, *123*, 11673.
(14) Tasis, D.; Tagmatarchis, N.; Bianco, A.; Prato, M. *Chem. Rev.* **2006**, *196*, 1105.
(15) Hirsch, A.; Vostrowsky, O. *Top. Curr. Chem.* **2005**, *245*, 193.
(16) Star, A.; Stoddart, J. F.; Steuerman, D.; Diehl, M.; Boukai, A.; Wong, E. W.; Yang, X.; Chung, S. W.; Choi, H.; Heath, J. R. *Angew. Chem., Int. Ed.* **2001**, *40*, 1721.
(17) Vigolo, B.; Penicaud, A.; Coulon, C.; Sauder, C.; Pailler, R.; Journet, C.; Bernier, P.; Poulin, P. *Science* **2000**, *290*, 1331.
(18) O'Connell, M. J.; Bachilo, S. M.; Huffman, C. B.; Moore, V. C.; Strano, M. S.; Haroz, E. H.; Rialon, K. L.; Boul, P. J.; Noon, W. H.; Ma, J.; Hauge, R. H.; Weisman, R. B. *Science* **2002**, *297*, 593.
(19) Tournus, F.; Latil, S.; Heggie, M. I.; Charlier, J.-C. *Phys. Rev. B: Condens. Matter Mater. Phys.* **2005**, *72*, 075431.
(20) Chen, J.; Liu, H.; Weimer, W. A.; Halls, M. D.; Waldeck, D. H.; Walker, G. C. *J. Am. Chem. Soc.* **2002**, *124*, 9034.

PFO-P
poly[(9,9-dioctylfluorenyl-2,7-diyl)-co-(1,4-phenylene)]

PFO
poly[9,9-dioctylfluorenyl-2,7-diyl]

PFO-PBAB
Poly[(9,9-dioctylfluorenyl-2,7-diyl)-co-(N,N'-diphenyl)-N,N'di(p-butyl-oxy-phenyl)-1,4-diaminobenzene)]

PFH
poly[9,9-dihexylfluorenyl-2,7-diyl]

PFO-BT
poly[(9,9-dioctylfluorenyl-2,7-diyl)-alt-co-(1,4-benzo-2,1',3-thiadiazole)]

MEHPPV
poly[2-methoxy-5-(2'-ethyl-hexyloxy)-1,4-phenylene vinylene]

Figure 1. Structures of the aromatic polymers used in this study.

between conjugated polymers and carbon nanotubes could enhance SWNT properties, for example, in nonlinear optics.[22] Also, the combination of polymers and carbon nanotubes has great potential for applications in photovoltaic devices,[23] light-emitting diodes,[24] and field-effect transistors.[25]

There have been a number of previous works on both the purification of SWNTs and the separation of specific species. Papadimitrakopoulos and co-workers[26] and Maeda et al.[27] have both reported successful large-scale separation of semiconducting and metallic SWNTs using weakly adsorbed amines. An alternative dispersing agent is DNA, whose helical structure has been reported to enclose and wrap SWNTs. This has been shown to efficiently narrow the diameter distribution of nanotubes.[28,29] It has also been suggested that a wrapping agent such as a conjugated polymer,[20,30,31] with structures having strong interactions with the surfaces of SWNTs through $\pi-\pi$ interactions, might result in the selective solubilization of SWNTs with certain diameters or chiral structures.

We have recently reported[32] that the use of nonaqueous solvents, combined with light-emitting aromatic polymers, can

lead to a very high degree of selectivity in terms of the nanotube species which are solubilized as isolated tubes. In addition, these polymers also show energy transfer from the polymer to the nanotubes,[33] providing a further route for nanotube excitation. In the present paper we present an extended description of this work, examining a further range of polymers and solvents, and demonstrate that the solvent plays a critical role in affecting the final distribution of dispersed SWNTs. We have studied optical absorption, sensitive to both bundled and isolated tubes, which demonstrates that the solubilization of nanotubes can be achieved with most of the processes studied here. Photoluminescence, which by contrast is only sensitive to isolated tubes, emphasizes the different distributions which occur for the different solvent/polymer combinations.

Experimental Section

The polymers poly[9,9-dioctylfluorenyl-2,7-diyl] (PFO), poly[9,9-dihexylfluorenyl-2,7-diyl] (PFH), poly[(9,9-dioctylfluorenyl-2,7-diyl)-co-(1,4-phenylene)] (PFO-P), poly[(9,9-dioctylfluorenyl-2,7-diyl)-co-(N,N'-diphenyl)-N,N'di(p-butyl-oxy-phenyl)-1,4-diaminobenzene)] (PFO-PBAB), and poly[(9,9-dioctylfluorenyl-2,7-diyl)-alt-co-(1,4-benzo-2,1',3-thiadiazole)] (PFO-BT) were purchased from American Dye Source, Inc. Poly[2-methoxy-5-(2'-ethyl-hexyloxy)-1,4-phenylene vinylene] (MEHPPV) was purchased from Sigma Aldrich. Schematic pictures of the polymer structures are shown in Figure 1. Solvents were purchased from Sigma Aldrich. Samples of SWNTs grown by the "HiPCO" growth process[34] were purchased from Carbon Nanotech., Inc. The nanotubes were used as purchased with quoted purities of >85% SWNTs. The solutions were prepared with the ratio 5 mg SWNT/6 mg polymer/10 mL solvent, then homogenized in a sonic bath

(21) Ogawa, K.; Zhang, T.; Yoshihara, K.; Kobuke, Y. *J. Am. Chem. Soc.* **2002**, *124*, 22.
(22) Wang, Z.; Liu, C.; Liu, Z.; Xiang, H.; Li, Z.; Gong, Q. *Chem. Phys. Lett.* **2005**, *407*, 35.
(23) Granstrom, M.; Petritsch, K.; Arias, A. C.; Lux, A.; Andersson, M. R.; Friend, R. H. *Nature* **1998**, *395*, 257.
(24) Friend, R. H.; Gymer, R. W.; Holmes, A. B.; Burroughes, J. H.; Marks, R. N.; Tailiani, C.; Bradley, D. D. C.; Dos Santos, D. A.; Bredas, J. L.; Logdlund, M.; Salaneck, W. R. *Nature* **1999**, *397*, 121.
(25) Sirringhaus, H.; Tessler, N.; Friend, R. H. *Science* **1998**, *280*, 1741.
(26) Chattopadhyay, D.; Galeska, I.; Papadimitrakopoulos, F. *J. Am. Chem. Soc.* **2003**, *125*, 3370.
(27) Maeda, Y. et. al. *J. Am. Chem. Soc.* **2005**, *127*, 10287.
(28) Zheng, M.; Jagota, A.; Semke, E. D.; Diner, B. A.; Mclean, R. S.; Lustig, S. R.; Richardson, R. E.; Tassi, N. G. *Nat. Mater.* **2003**, *2*, 338.
(29) Zheng, M.; Diner, B. A. *J. Am. Chem. Soc.* **2004**, *126*, 15490.
(30) Rice, N. A.; Soper, K.; Zhou, N.; Merschrod, E.; Zhao, Y. *Chem. Commun.* **2006**, 4937.
(31) Wei, C. *Nano Lett.* **2006**, *6*, 1627.

(32) Nish, A.; Hwang, J.-Y.; Doig, J.; Nicholas, R. J. *Nat. Nanotechnol.* **2007**, *2*, 640.
(33) Nish, A.; Hwang, J.-Y.; Doig, J.; Nicholas, R. J. *Nanotechnology* **2008**, *19*, 095603.
(34) Nikolaev, P.; Bronikowski, M. J.; Bradley, R. K.; Rohmund, F.; Colbert, D. T.; Smith, K. A.; Smalley, R. E. *Chem. Phys. Lett.* **1999**, *313*, 91.

for 60 min to achieve maximum solubility followed by vigorous sonication using an ultrasonic disintegrator for 15 min in order to debundle the nanotubes and make them optically active. Longer sonication times did not improve the optical activity of the solutions.[33] This was then promptly followed by centrifugation at 9000g for 3 min. The preparation used for dispersions in sodium dodecylbenzene sulfonate (SDBS), used here for comparison with polymers, consisted of 5 mg SWNT/350 mg surfactant/35 mL D$_2$O. Sonication was for 30 min using an ultrasonic disintegrator, and centrifugation was performed with an ultracentrifuge at 85 000g for 4 h. Absorbance measurements were taken using a Perkin-Elmer UV−vis−near-infrared spectrophotometer (Lambda 9). Photoluminescence excitation (PLE) mapping was done using an automated custom-built system consisting of a 75 W xenon lamp focused into a monochromator which then illuminated the samples in a quartz fluorescence cell. Normalization for the lamp's spectral response was done using a silicon photodiode. Luminescence from the samples was collected at an angle 90° to the excitation beam and focused into a spectrograph fitted with a liquid-nitrogen-cooled InGaAs photodiode array. Raman measurements were performed at room temperature using a Kr$^+$ laser at 647 nm for excitation and a Jobin-Yvon T64000 triple-grating spectrometer with a nitrogen-cooled multichannel CCD detector. The transmission electron microscopy (TEM) and atomic force microscopy (AFM) image studies were conducted by JEOL 4000EX and ThermoMicroscope M5 instruments, respectively.

Results

Absorbance. Optical absorbance studies were performed on all the nanotube solutions prepared. All solutions use the same starting HiPCO SWNT material and might be expected to show similar optical properties, if the solubilization process is independent of tube species. The absorbance spectra in this work are dominated by the absorption of the E$_{11}$ and E$_{22}$ bands of the semiconducting SWNTs in the wavelength region from 500 to 1600 nm. The absorption intensity is proportional to the amount of solubilized nanotubes, independent of whether they are isolated or bundled and contrasts with photoluminescence (PL), where only isolated semiconducting tubes contribute intensity. Figure 2a shows the absorbance spectra of SWNTs dispersed in the range of polymers studied using the solvent toluene. Some spectra have been magnified for comparison (the dramatic increase in the short wavelength region is due to the onset of polymer absorption). All solutions were prepared with the same process parameters, including starting concentration, sonication power and time, and centrifugation conditions. Absorbance was measured in a quartz cell using the same path length and corrected with a toluene reference solution. Figure 2a shows the magnitude of the optical absorbance to be highly sensitive to the structure of the polymer. Polymer solutions which have high total absorbance, such as PFO-P and MEHPPV, also show less well-resolved features, due to the presence of multiple overlapping peaks, while those with lower total absorbance, such as PFH and PFO-BT, are much narrower and better resolved. These resolved features may be correlated with the peaks observed in PLE maps, examples of which will be shown later. This indicates that as solubilizing agents, the polymers have varying degrees of selectivity at dispersing SWNTs and also that polymers showing a high selectivity, such as PFO−BT, only disperse a smaller fraction of the nanotubes present.

Figure 2b shows how the choice of solvent affects the dispersion for PFO in three organic solvents: toluene, THF, and chloroform. Also shown is the absorbance spectrum of SWNTs dispersed in aqueous solution using the ionic surfactant
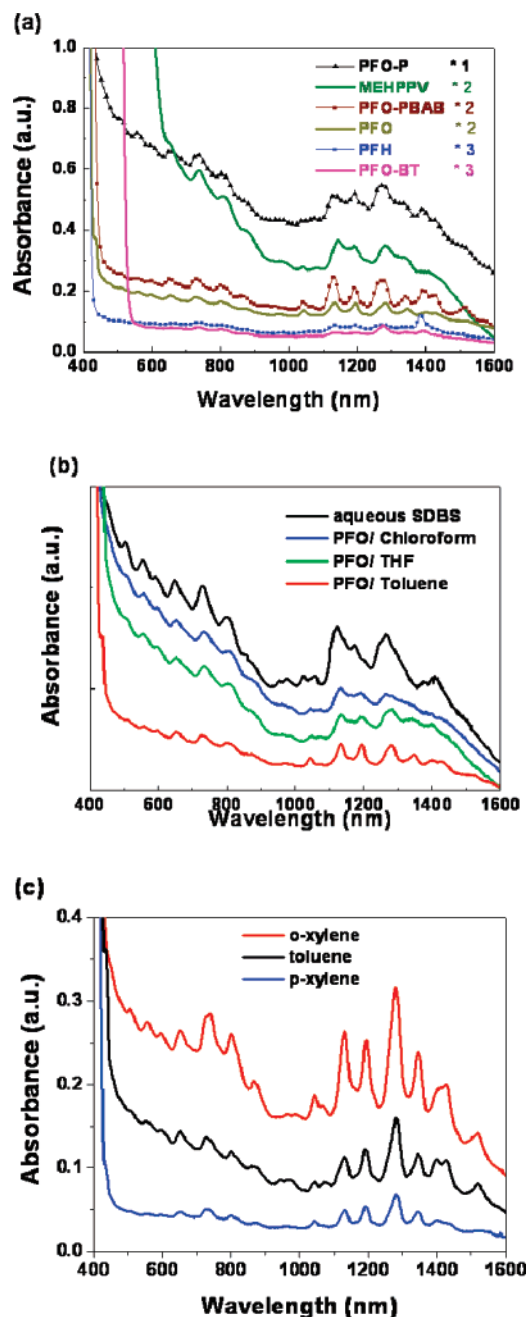
Figure 2. (a) Absorbance spectra of dispersed HiPCO-produced SWNTs with different polymers using toluene solvent; (b) spectra of dispersed nanotubes using PFO in the solvents toluene, THF, and chloroform compared with that prepared in SDBS aqueous solutions; (c) spectra of dispersed nanotubes using PFO in the solvents toluene, *p*-xylene, and *o*-xylene.

SDBS, which is thought to disperse SWNTs without any selectivity. These spectra have been adjusted for visual comparison because the spectra of solutions in THF and chloroform are only measurable when the solutions are diluted, due to the very high solubilization of the nanotubes. All polymer solutions prepared with THF and chloroform showed similarly high solubilizations, typically 2 to 3 orders of magnitude greater than that in toluene. In general, the polymer/chloroform solutions show the highest nanotube solubility, THF shows the second-highest solubility, and toluene shows the lowest solubility. The higher solubility is associated with all SWNT species being solubilized, hence, yielding the poorly resolved absorption
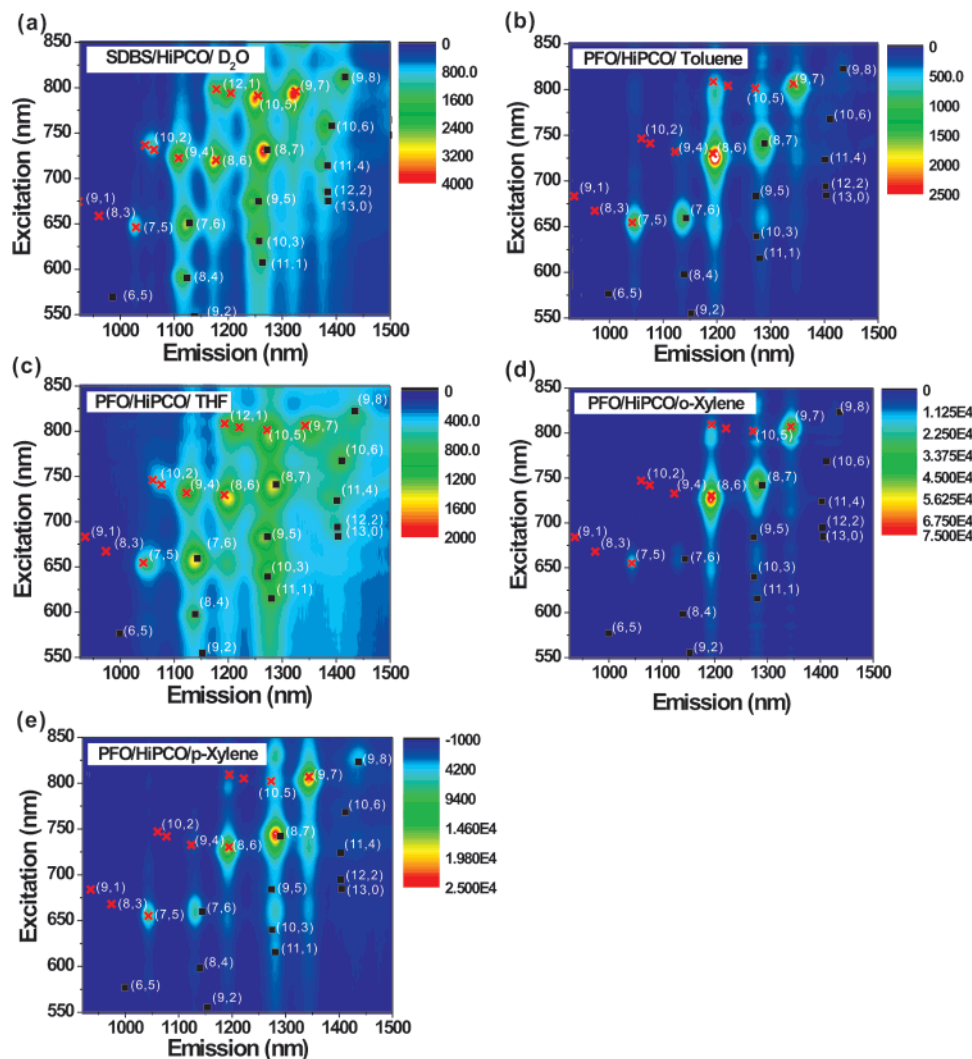
Figure 3. PLE maps where the false color scale represents the intensity of emission from SWNTs dispersed using SDBS in aqueous solution and using PFO in the organic solvents THF, toluene, *o*-xylene, and *p*-xylene. The points represent the positions of SWNT resonances using the scheme proposed by Weisman and Bachilo.[33]

features. By contrast, absorbance measured using the family of solvents *o*-xylene, toluene, and *p*-xylene, which have much more similar properties, show (Figure 2c) very similarly resolved spectra but still have a difference in absorbance of a factor of more than 3.

Photoluminescence-Excitation (PLE). Photoluminescence spectroscopy[7,18] is particularly sensitive to isolated nanotubes since their aggregation into bundles not only quenches the luminescence but also causes broadening of the optical transitions. This is due to the interaction with other nanotube species and, in particular, to metallic tubes which provide efficient nonradiative decay pathways for any photoexcited carriers. Figure 3 shows the PLE maps of SWNTs dispersed using SDBS in aqueous solution and using PFO in the organic solvents toluene, THF, *o*-xylene, and *p*-xylene. The peaks correspond to resonant emission from the primary E_{11} electronic transitions when the excitation matches the secondary E_{22} electronic levels.[18] The points indicate the empirical positions for the energy gaps of the corresponding (*n*,*m*) indexed tube species given by Weisman et al. for the case of SWNTs dispersed using an aqueous surfactant,[35] but with a red shift of approximately 1.3%. This is due to the surrounding polymers causing a difference in the local dielectric environment where the increased

dielectric screening causes a reduction of the electron−electron and excitonic Coulomb interactions.[36−38] This shift varies slightly between different polymers, but is independent of the solvent used. Other resonant features which are visible at higher and lower energy excitation relative to E_{22} also result in emission from the same E_{11} energy gaps and can be attributed to previously established phonon[39] and weakly allowed absorption[40] effects.

The peaks in Figure 3a for the aqueous SDBS solution correspond to a typical distribution of standard HiPCO-produced SWNTs, with 23 species observed. For the same SWNT material prepared using PFO and organic solvents, totally different results are found. Only 6 peaks may be observed in PFO/toluene (Figure 3b), almost all (22) peaks are detected in PFO/THF

(35) Weisman, R. B.; Bachilo, S. M *Nano Lett.* **2003**, *3*, 1235.
(36) Ando, T. *J. Phys. Soc. Jpn.* **2004**, *73*, 3351.
(37) Li, L.-J.; Lin, T.-W.; Doig, J.; Mortimer, I. B.; Wiltshire, J. G.; Taylor, R. A.; Sloan, J.; Green, M. L. H.; Nicholas, R. J. *Phys. Rev. B: Condens. Matter Mater. Phys.* **2006**, *74*, 245418.
(38) Li, L. J.; Khlobystov, A. N.; Wiltshire, J. G.; Briggs, G. A. D.; Nicholas, R. J. *Nat. Mater.* **2005**, *5*, 481.
(39) Jones, M.; Engtrakul, C.; Metzger, W. K.; Ellingson, R. J.; Nozik, A. J.; Heben, M. J.; Rumbles, G. *Phys. Rev. B: Condens. Matter Mater. Phys.* **2005**, *71*, 115426.
(40) Miyauchi, Y.; Oba, M.; Maruyama, S. *Phys. Rev. B: Condens. Matter Mater. Phys.* **2006**, *74*, 205440.

Table 1. Relative Intensity of SWNT Species Deduced from PLE Maps of Samples Prepared in SDBS Aqueous Solutions and Polymers/Toluene

|				relative intensity (%)						
				D$_2$O	toluene					
(n,m)	q	diameter (nm)	chiral angle (deg)	SDBS	PFO-P	PFO-PBAB	PFO	MEHPPV	PFH	PFO-BT
(7,5)	−1	0.829	24.50	28.42	18.81	31.22	38.99	33.31	24.34	
(7,6)	1	0.895	27.46	70.19	41.67	100	34.60	86.44	37.01	
(8,4)	1	0.840	19.11	35.08	18.46	24.49				
(8,6)	−1	0.966	25.28	85.95	73.43	98.68	100	100	75.28	5.8
(8,7)	1	1.032	27.80	87.85	71.53	86.00	46.43	76.16	100	26.25
(9,4)	−1	0.916	17.48	68.14	67.99	25.71		86.81	28.11	10.47
(9,5)	1	0.976	20.63	49.74	71.35	47.95		59.69	36.39	
(9,7)	−1	1.103	25.87	100	73.68	62.10	47.02	57.59	97.99	16.67
(9,8)	1	1.170	28.05	43.76	51.60	37.37	8.62			
(10,2)	−1	0.884	8.95	16.08	36.96					
(10,3)	1	0.936	12.73	24.92	29.68	8.29		19.69	16.94	
(10,5)	−1	1.050	19.11	86.66	100	27.85		68.48		100
(10,6)	1	1.111	21.79	44.31	56.43	22.83		30.03		7.5
(10,8)	−1	1.240	26.33	14.63	30.20					
(11,0)	−1	0.873	0.00	15.98	13.72					
(11,1)	1	0.916	4.31	12.32	16.05	3.90				
(11,3)	−1	1.014	11.74	58.39	29.51			42.79	37.64	
(11,4)	1	1.068	14.92	27.43	32.44	14.63		16.47		8.63
(11,6)	−1	1.186	20.36	30.84	55.05	11.32				
(12,1)	−1	0.995	3.96	31.86	43.83			36.16	36.64	
(12,2)	1	1.041	7.59	13.47	22.09	9.17		13.99		9.07
(12,4)	−1	1.145	13.90	48.97	43.05	9.76				
(12,5)	1	1.201	16.63	19.41						
(13,2)	−1	1.120	7.05	41.03	23.73	11.76				9.21
(13,3)	1	1.169	10.16	15.36						

(Figure 3c), and in the case of PFO/chloroform, no SWNT photoluminescence could be observed at all. From the increased solubility using PFO/chloroform seen in the absorbance spectra, coupled with the absence of photoluminescence, we may conclude that the dispersed SWNTs remain mostly bundled. Any isolated nanotubes suspended cannot be detected as the exciting or emitted light may be absorbed by the large amount of nonemissive suspended material. Figure 3d,e shows that in agreement with the absorption measurements, *o*-xylene and *p*-xylene show similar peaks to those observed for toluene, with the strongest emission coming from the *o*-xylene solvent solution. In order to perform a systematic study, therefore, solutions were prepared for all other polymers using toluene, chloroform, and THF. PLE maps for the toluene and THF solutions were recorded, while none of the solutions using chloroform show any photoluminescence.

To compare the PLE results of different polymer/solvent combinations quantitatively, we first calculate the intensity of each peak using peak-fitting software. Fitting procedures along both the excitation and emission axes have to be considered so that the overlap of peaks and contributions from phonon effects may be removed. In order to ensure that all PLE maps measured have a good signal-to-noise ratio, particularly important for detecting the minority species, the parameters of the measurements were separately optimized for each solution. Therefore, for each PLE map the fitted intensity is normalized by the species which shows the highest intensity and represented as a percentage. Examples of the calculated results are shown in Table 1. The data are presented graphically in schematic representations called graphene sheet maps[41] and histograms of the PL intensity as a function of diameter and chiral angle.

(41) Weisman, R. B.; Bachilo, S. M; Tsyboulski, D. *Appl. Phys. A* **2004**, *78*, 1111.

A sample graphene sheet map is shown in Figure 4 for the reference aqueous SDBS solution. Each hexagon corresponds to one (n,m) indexed carbon nanotube species and is shaded in a grayscale from white to black, proportional to its relative intensity, according to the values given in Table 1. Histograms of the photoluminescence are also plotted for the relative intensity against the nanotube diameter or chiral angle. The illustrations of Figure 4 show that the HiPCO-produced SWNTs used have a fairly wide distribution of diameters, between 0.8 and 1.25 nm, and of chiral angles from 0 to 30°. No correction has been made for possible differences in the quantum efficiencies of different species. However, the even distribution of chiral indices shown suggests that this is not a strong function of the nanotube parameters.

Figure 5 shows the graphene sheet maps of the SWNTs dispersed using the different polymers in toluene (left) and THF (right), and Figure 6 shows the histograms as a function of diameter (left) and chiral angle (right). The distribution of dispersed species is strongly dependent on both polymer and solvent, although some general observations can be made. First, the total number of species giving photoluminescence is usually higher in THF than in toluene. This is probably related to the higher overall solubility of SWNTs in THF, as shown in Figure 1, for PFO, PFH, and PFO-BT. By contrast, although PFO-P and PFO-PBAB have a relatively high absorption intensity in THF, the number of species present is found to decrease, which we attribute to the THF solutions preferentially selecting smaller diameter tubes. For example, the strongest species in PFO-P/toluene and PFO-BT/toluene are both (*10,5*) but shift to (*9,4*) when THF is used. It is thought that the change of solvent environment alters the polymer conformation and thus affects the interaction, or binding energy, between the polymer and specific SWNT species. For the case of MEHPPV, with a very
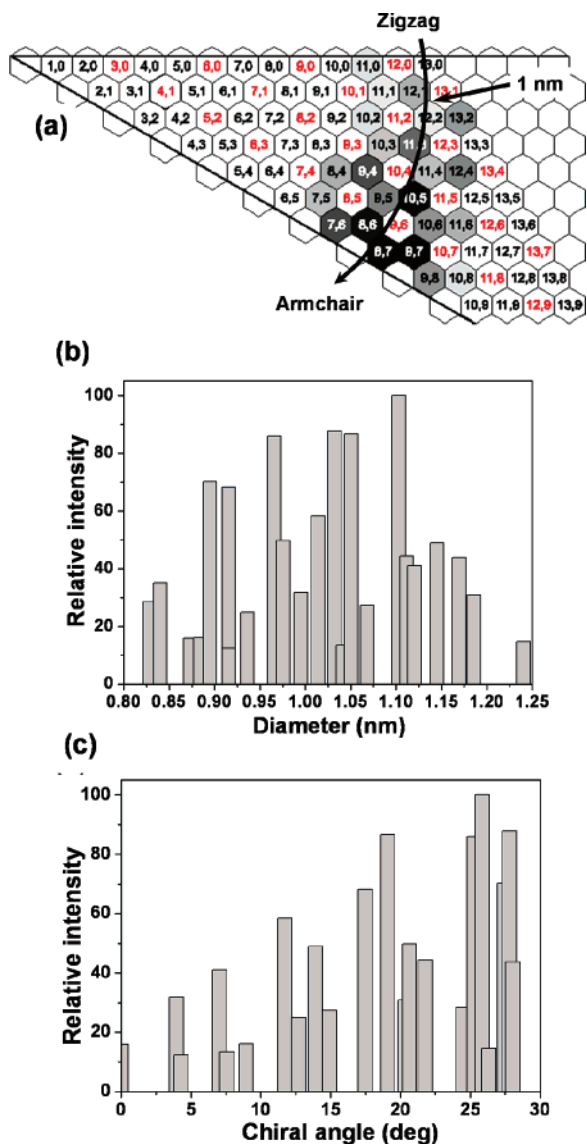
Figure 4. Schematic representations of SWNT solutions using aqueous SDBS as a dispersing agent. Shown is a graphene sheet map (a) and histograms for distributions with respect to diameter (b) and chiral angle (c).

different structure from the other polymers studied in this work, the behavior of the two solvents is reversed, with toluene showing a reduced number of nanotubes solubilized and a preference for smaller diameters.

Comparing the species-specific actions of the different polymer/solvent combinations, we may divide these into four groups:

(1) Species specific. The most remarkable combination is PFO-BT (Figure 6f) in toluene, which selects the (*10,5*) species to such a strong extent that it is more than 4 times stronger than any other. In THF, PFO-BT also shows a significant preference, but now for the (*9,4*) species, but a significant number of other tubes remain and so it is included in the third group of diameter-selective treatments. PFO/toluene (Figure 6d) might also be included in this group, although its main action seems to be through its chiral angle selectivity. Nevertheless, when combined with a different starting material such as nanotubes produced by the CoMoCAT process, it is capable of producing solutions[32] with over 50% of the single species (*7,5*).

(2) Chirality preference. PFO/toluene has a very strong dependence on the chiral angle of SWNTs in favor of near-armchair structures, but this phenomenon disappears using THF. Both PFH (Figure 6e) and PFO-PBAB (Figure 6b) also show significant chiral selectivity in both toluene and THF solutions, although the toluene is still better.

(3) Diameter preference. In THF solutions, PFH, PFO-BT, and PFO-P (Figure 6a) all show a preference for tube diameters in the range of 0.9–1.05 nm, which is significantly narrower than the original starting material, while a similar behavior is seen with MEHPPV/toluene (Figure 6c), but not with THF.

(4) No particular preference. In toluene, PFO-P, and in THF, PFO and MEHPPV, show no apparent preference, but solubilize all nanotubes well.

Raman Scattering. Raman scattering may also be used to demonstrate the enhanced selectivity which occurs as a function of solvent and has the advantage of not being strongly influenced by the bundling state of the nanotubes. The radial breathing mode (RBM) frequencies are proportional to 1/diameter of the nanotubes[42] and show resonances similar to those seen in the PLE spectra. RBM spectra are shown in Figure 7 taken using an excitation wavelength of 647 nm which is in resonance[33,42] with the (*10,3*), (*7,6*), (*7,5*), and (*8,3*) semiconducting nanotubes and a group of metallic nanotubes with diameters of ∼1.2 nm which give a broad peak at around 200 cm^{-1}. The spectra are normalized to the strength of the (*7,5*) peak. The strength of the metallic peak is quite significantly reduced when PFO is used with all of the organic solvents, even chloroform, and the additional selectivity which occurs for the PFO/toluene combination results in almost total removal of all of the metallic species, as reported previously.[32]

TEM and AFM. Figure 8 shows the TEM and AFM images of SWNTs dispersed using PFO in toluene and chloroform. In the case of PFO/toluene, the TEM images often show composite structures 6–7 nm across showing only one SWNT surrounded by polymer, marked with an arrow as indicated in Figure 8a. The presence of the polymer makes it difficult to image the nanotube side wall due to the overlap of polymer matrix. The low magnification images (inset) suggest there are some composites with larger sizes. However this may be due to aggregation caused during the preparation of the samples for TEM. In contrast, the nanotube/polymer composites in PFO/chloroform solutions are larger and denser, often overlapping and interwoven, as shown in the inset of Figure 8b. Most of the composites are larger than 10 nm across and usually contain multiple nanotubes wrapped together by polymer, as marked in Figure 8b. These images support the conclusions from the optical measurements that although the polymers have successfully wrapped and dispersed nanotubes in chloroform, the dispersed nanotubes remain bundled.

The AFM study further confirms the TEM results. The drop-cast films from the toluene solutions have nanotube-rich and polymer-rich areas, but those from chloroform solutions form very thick, black films. Figure 8c shows the nanotube-rich area from a toluene solution, with very uniformly dispersed wires, each with height of around 6 nm as seen in TEM. This is the size of the single tube wrapped by PFO observed in TEM. For the chloroform solution films, images are shown in Figure 8d

(42) Jorio, A.; Saito, R.; Hafner, J. H.; Lieber, C. M.; Hunter, M.; McClure, T.; Dresselhaus, G.; Dresselhaus, M. S. *Phys. Rev. Lett.* **2001**, *86*, 1118.
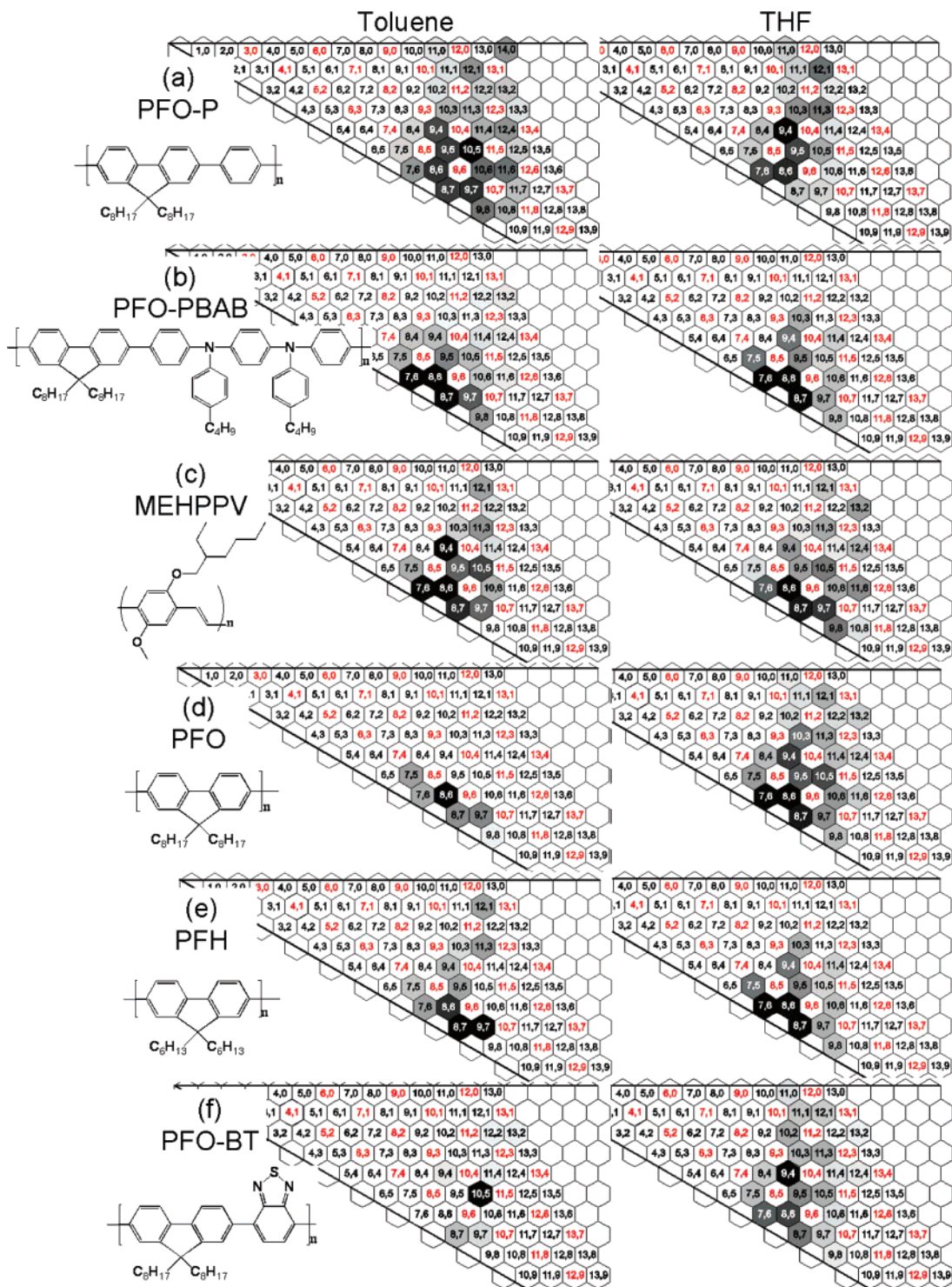
Figure 5. Graphene sheet maps showing normalized PL intensity of SWNTs dispersed using various polymers, whose structures are also shown, in toluene (left) and THF (right).

for both the dense central area and area close to an edge. In the central area, the features are typically in the order of tens of nanometers high, corresponding with the TEM results, but at the edges some individual tubes without any polymer wrapping and some smaller size composites are also found. These were probably not detected optically due to the low total fluorescence quantum yield of the solutions and the parasitic absorption of bundles.

Molecular Dynamics Simulation. In order to understand the polymer structure and effect of the solvent on the selectivity

and solubility of the polymers as SWNT dispersing agents, we have performed molecular mechanics simulations[43] using the MM3 force field.[44] We have previously shown[32] that the polymer PFO forms relatively rigid and rodlike chains, which simplifies the simulation process. Here we find several possible conformations where PFO surrounds a nanotube, some examples of which are shown in Figure 9a,b, with each having different binding energies between the PFO and nanotube. These different

(43) Ponder, J. W.; Richards, F. M. *J. Comput. Chem.* **1987**, *8*, 1016.
(44) Allinger, N. L.; Yuh, Y. H.; Lii, J. H. *J. Am. Chem. Soc.* **1989**, *111*, 8551.
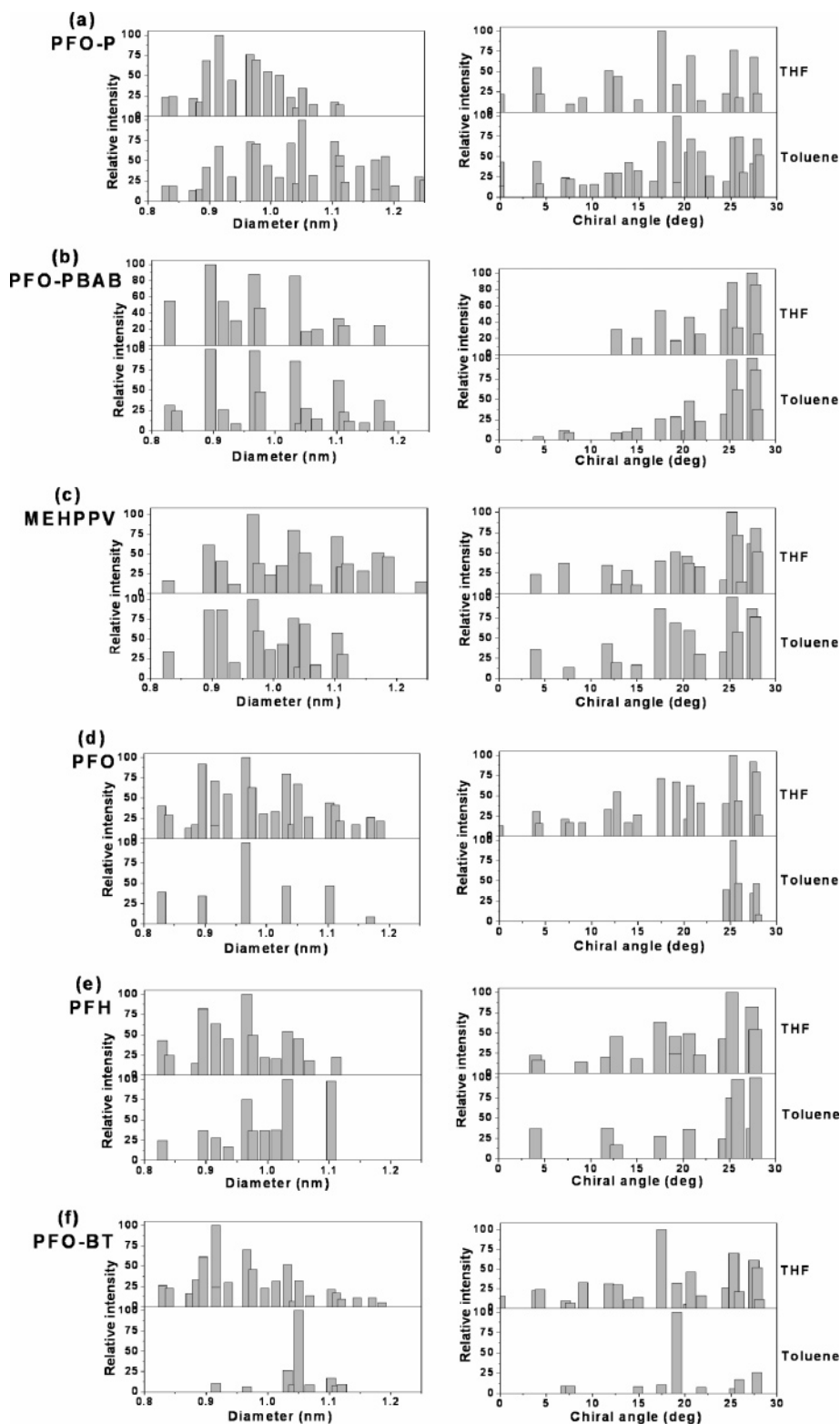
Figure 6. Histograms of dispersed SWNTs using polymers in toluene (lower diagrams) and THF (upper diagrams) show chiral angle and diameter distribution.

conformations might be stable in different solvent environments, therefore causing the observed solubilization and selective dispersion effects. Figure 9a shows wrapping mainly by side chains of PFO, while the wrapping through the $\pi-\pi$ interactions between nanotubes and the backbone of PFO is also possible as shown by the structure in Figure 9b. Another possibility occurs when all the side-chain groups are on the same side. This can cause the backbone to twist around the tube, as shown

in Figure 9c for a (*10,5*) tube and PFO-P, whose unit structure is a copolymer of PFO with a benzene ring. This extra benzene ring gives the polymer backbone more freedom to rotate and fit the curvature of the SWNT surface.

Discussion

The optical studies above show that the total solubility and the selectivity of dispersed nanotubes are highly dependent on
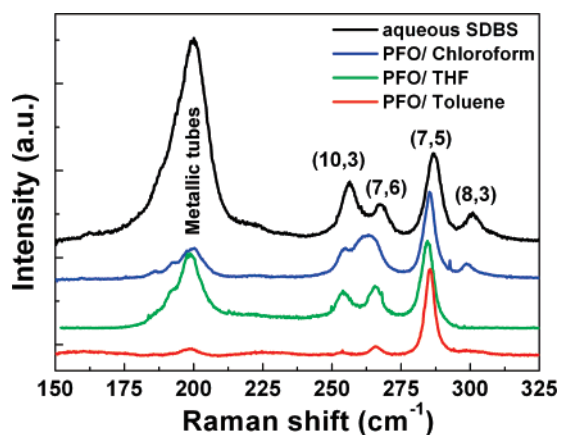
Figure 7. Raman spectra of the RBM frequencies of SWNTs dispersed in aqueous SDBS and PFO/organic solvents excited at 647 nm using a Kr⁺ laser.

the polymer structures and solvents. There is a considerable volume of literature on how solvents affect the conformation of polymers and affect their physical properties.[45−47] The solubility of polymers, reflecting their conformation, is sensitive to several different solvent parameters: polarity, aromaticity, and solvent architecture.[48] When polymers are in an unfavorable solvent, they tend to fold and minimize exposure to the solvent, and in a favorable solvent, they have a relatively open and straight conformation. As a result it is generally believed that the solubility of SWNTs is related to the density and polarity of the solvents used. Solvents with high density or high polarity will cause high solubility of SWNTs. Liu et al. used two different solvents for poly(2,7-9,9(di(oxy-2,5,8-trioxadecane))-fluorene), which has very similar structure to PFO, to disperse SWNTs.[49] They described a simple model and suggested that the polarity of the solvents will strongly affect the way the polymers aggregate and thus influence the degree of dispersion of the nanotubes. This is confirmed by the absorption data of Figure 2c where the higher polarity *o*-xylene shows a much higher solubility than *p*-xylene. Bahr et al.[50] used several organic solvents to solubilize SWNTs without any surfactant and compared their solubility. Chloroform has solubility of 31 mg/L, THF has a solubility of 4.9 mg/L, and the solubility of toluene is less than 1 mg/L after 1 h of sonication followed by filtration through glass wool. Here, the presence of the polymer makes a similar measurement unreliable, but the absorbance spectra suggest that the solubility of SWNTs in the same three solvents is consistent with the observation made by Bahr et al.

Solvent density is also of some importance. It has been reported by Arnold et al.[51] that it is possible to sort SWNTs species by density differentiation using extended ultracentrifugation of aqueous solutions. Since the technique we use to prepare SWNT solutions includes centrifugation, aggregations of polymers and SWNTs of higher relative density to the solvents are sedimented to the bottom of centrifuge tubes.[18] The density of chloroform, however, is 1.5 g/cm³, much higher than those of D₂O, 1.1 g/cm³, and THF and toluene, 0.9 g/cm³. This high density helps to suspend the SWNTs through buoyant forces, either bundled or debundled, even without the surfactant. The high solvent density is thought to be responsible for the sizable amount of polymer-wrapped bundled nanotubes which exist in chloroform solutions, as confirmed by the TEM and AFM studies. By contrast, large differences occur in the species preferred in dispersions using THF and toluene, which have almost the same density, but have very different polarity and structure. This is evidence that the changes in conformation and aggregation of the polymers caused by the solvents play an important role in the observed behavior.

Many reports exist in the literature of molecules with aromatic rings adsorbed on SWNTs through $\pi-\pi$ interactions.[52,53] The $\pi-\pi$ stacking between aromatic molecules and the surface of SWNTs is likely to exhibit a preferred specific orientation. This may be the reason why these aromatic polymers have such a strong selectivity. If a specific nanotube species with a particular surface structure fits the stacking with the polymer backbone, the amount of this species solubilized will be enhanced. When the diameter of the nanotube is reduced, this stacking effect will become more sensitive because the curvature of the graphene surfaces of SWNTs becomes larger and thus makes the stacking conditions more critical.

The intrinsic structure of PFO greatly limits the possibility of conformation changes. This enhances its selectivity because the effect of the $\pi-\pi$ stacking of the PFO backbone and nanotube surface dominate the binding energy between the PFO and nanotubes. Furthermore, the length of the side groups influences the solubility of the SWNTs since longer side chains will cover more nanotube surface area and result in stronger composite structures. PFH, with side groups shorter by two carbon atoms compared with PFO, shows much lower SWNT solubility than PFO. However, these two polymers both show highly selective dispersion of SWNTs due to the limitations of conformation. Where more freedom of conformation exists, the selectivity decreases. PFO-P, with its backbone extended by an extra benzene ring, has increased flexibility of the polymer chains and shows nonselective dispersion. PFO-PBAB and PFO-BT both have an extended backbone similar to that of PFO, but the unique side groups complicate the conformation conditions compared with PFO-P, therefore affecting the resultant dispersions.

MEHPPV is also an aromatic polymer but with a very different structure from the others used here, making it an interesting comparison to the PFO-based polymers. First, the absorption intensity of SWNTs in MEHPPV/toluene is between that of PFO-P/toluene and PFO-PBAB/toluene, but the number of species showing photoluminescence is somewhat less than that in PFO-PBAB/toluene. Second, when THF is used as a solvent in place of toluene, the total SWNT emission is found to increase for the case of MEHPPV in contrast to the decrease seen while using PFO-PBAB. Third, a shift in the solubilization

(45) Huser, T.; Yan, M.; Rothberg, L. J. *Proc. Natl. Acad. Sci. U.S.A.* **2000**, *97*, 11187.
(46) Schwartz, B. J. *Annu. Rev. Phys. Chem.* **2003**, *54*, 141.
(47) Quan, S.; Teng, F.; Xu, Z.; Qian, L.; Hou, Y.; Wang, Y.; Xu, X. *Eur. Polym. J.* **2006**, *42*, 228.
(48) Traiphol, R.; Sanguansat, P.; Srikhirin, T.; Kerdcharoen, T.; Osotchan, T. *Macromolecules* **2006**, *39*, 1165.
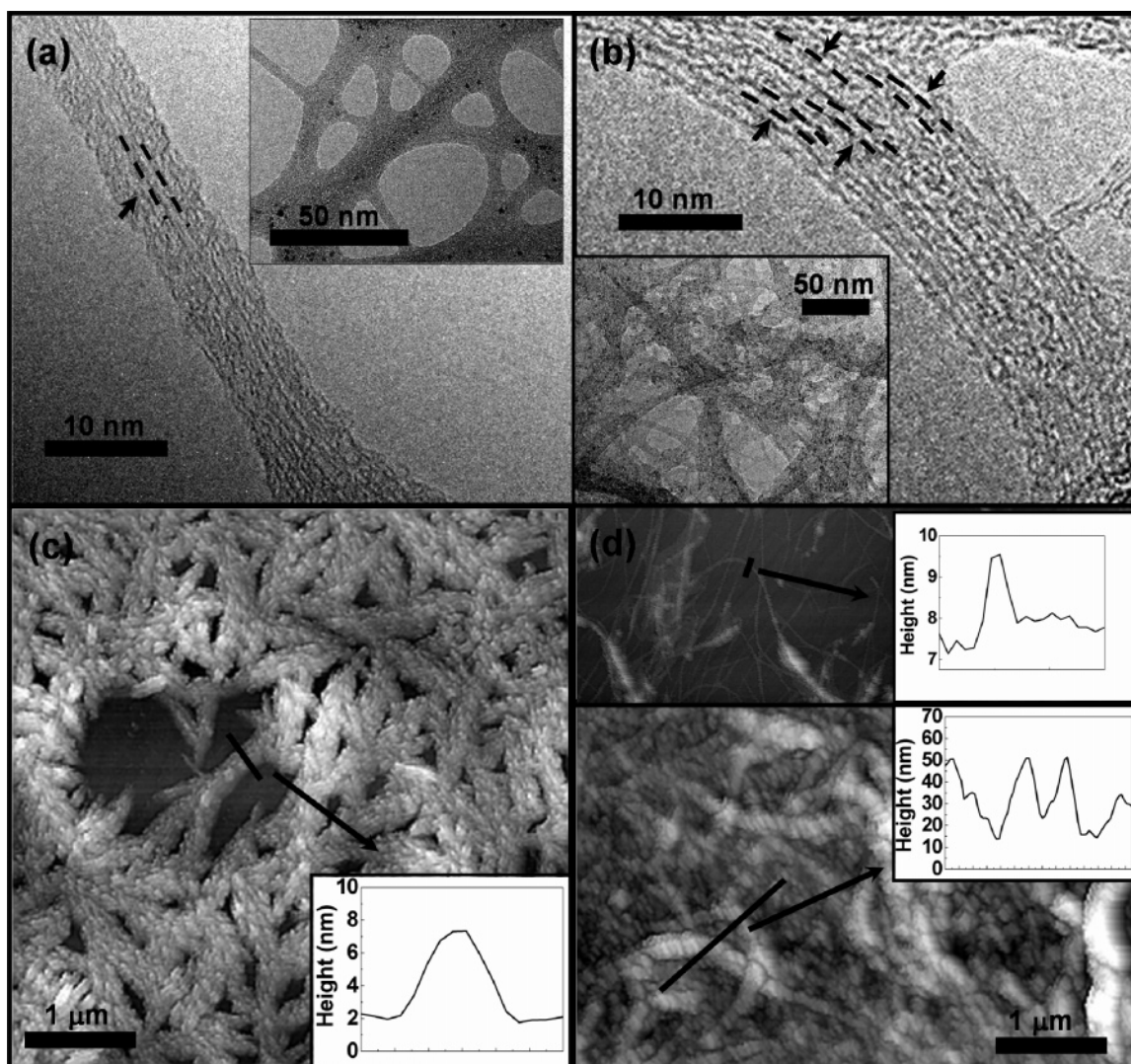(49) Liu, G.; Johnson, S.; Kerr, J. B. *Mater. Res. Soc. Symp. Proc.* **2004**, *796*, V6.8.1.
(50) Bahr, J. L.; Mickelson, E. T.; Bronikowski, M. J.; Smalley, R. E.; Tour, J. M. *Chem. Commun.* **2001**, 193.
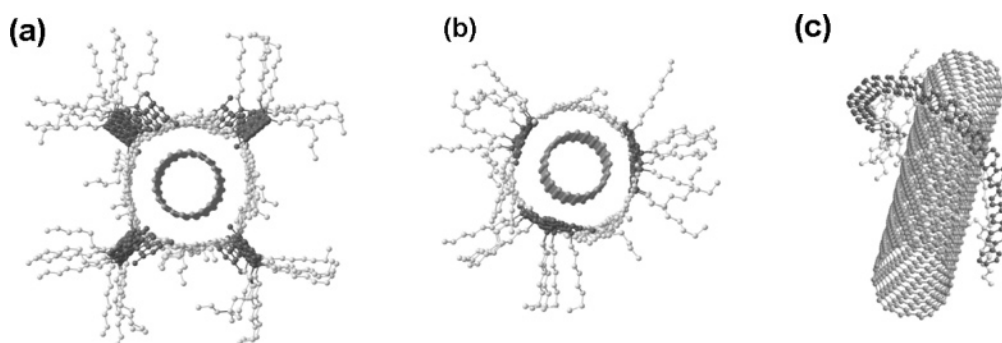(51) Arnold, M. S.; Green, A. A; Hulvat, J. F.; Strupp, S. I.; Hersam, M. C. *Nat. Nanotechnol.* **2006**, *1*, 60.

(52) Zhao, J.; Lu, J. P. *Appl. Phys. Lett.* **2003**, *82*, 3746.
(53) Gotovac, S.; Honda, H.; Hattori, Y.; Takahashi, K.; Kanoh, H.; Kaneko, K. *Nano Lett.* **2007**, *7*, 583.

Figure 8. TEM images of SWNTs dispersed using PFO in toluene (a) and chloroform (b) and AFM images of those in toluene (c) and chloroform (d).

Figure 9. Computer models of SWNTs wrapped by polymers. (a) (*10,0*) Tube surrounded by four PFO chains with their side-chain groups. (b) (*10,0*) Tube wrapped by three PFO chains through $\pi-\pi$ interaction between the PFO backbone and the nanotube surface. (c) (*10,5*) Tube helically wrapped by PFO-P with all the side-chain groups at one side. The darker atoms indicate the backbone of polymers.

to small diameter SWNTs is observed in most of the PFO-based polymers when THF is used in place of toluene. In the case of MEHPPV, the opposite behavior is seen. This is further evidence of how the polymer structure affects the solubilization of individual nanotubes in different solvents and shows that changes in polymer structure can drastically alter the results.

Conclusions

SWNTs have been successfully dispersed using aromatic organic polymers in various solvents. The solubility and the selective dispersion have been found to be strongly influenced by the polymer structures and solvent used. Chloroform gives the highest solubility for SWNTs, but evidence suggests that

most of the dispersed nanotubes are bundled. In toluene, the solubility of SWNTs is low. However, this enhances the possibility of selective dispersion of individual SWNTs, and depending on which polymers are used, this selectivity may be varied. When the limits on conformation increase, the selectivity increases, possibly due to increased $\pi-\pi$ stacking with a strong orientation preference. By the use of different combinations of conjugated polymers and solvents, it is not only possible to prepare SWNT solutions with different solubility but also to perform selective solubilization of SWNTs with the ability to selectively tune the distribution of nanotube species which are solubilized.

Supporting Information Available: Complete ref 27. This material is available free of charge via the Internet at http://pubs.acs.org.

JA0777640